

Electronic Supplementary Material for

Boosting the Electrocatalytic Hydrogen Evolution and Sodium-Storage Properties of Co₉S₈ Nanoparticles via the Encapsulation with Nitrogen-Doped Few-Layer Graphene Networks

Lizhi Qian,^a Zhiqiang Wei,^a Tingli Yu,^a Bingdong Chang,^b Zhiyuan Wang,^{a, c, d} Yanguo Liu,^{a, c, d, *}

Hongyu Sun,^{c, *} Wei Huang^{e, *}

^a School of Materials Science and Engineering, Northeastern University, Shenyang 110819, China

^b DTU Nanolab, National Centre for Nano Fabrication and Characterization, Technical University of Denmark, Kongens Lyngby 2800, Denmark

^c School of Resources and Materials, Northeastern University at Qinhuangdao, Qinhuangdao 066004, China

^d Key Laboratory of Dielectric and Electrolyte Functional Material Hebei Province, Northeastern University at Qinhuangdao, Qinhuangdao 066004, China

^e Department of Chemistry, Technical University of Denmark, Kongens Lyngby 2800, Denmark

* Corresponding authors.

E-mail addresses: weihua@kemi.dtu.dk (W. Huang), hyltsun@gmail.com (H. Sun),
lyg@neuq.edu.cn (Y. Liu)

1. Experimental section

1.1. Materials synthesis

ZIF-67 crystals were synthesized by a direct precipitation way. Cobalt(II) nitrate hexahydrate ($\text{Co}(\text{NO}_3)_2 \cdot 6\text{H}_2\text{O}$, 4 mmol) and 2-methylimidazole (20 mmol) were dissolved with methanol (30 mL) to form homogeneous solutions by sonication treatment. Then the 2-methylimidazole solution was poured into the $\text{Co}(\text{NO}_3)_2 \cdot 6\text{H}_2\text{O}$ solution, which was aged for 20 h at room temperature. ZIF-67 crystals were collected by centrifugation and subsequent drying at 80 °C for 5 h. For the synthesis of CS@NFLG networks, ZIF-67 crystals (0.1 g) and sublimed sulfur powder (0.1 g) were thoroughly mixed and put into the center of a tube furnace. The mixture was heated up to 600 °C for 2 h, and then cooled to room temperature automatically. During the whole process, argon gas with a flow rate of 50 mL min^{-1} was maintained. When the temperature reached to 600 °C, an oxygen gas with a flow rate of 0.1 mL min^{-1} was introduced into the argon to etch the carbon layer. For the synthesis of CS/rGO, graphene oxide (GO) powder was firstly prepared from the graphite by a modified Hummers method. The GO powder (60 mg) was dispersed in de-ionized water (30 mL), and then $\text{Co}(\text{NO}_3)_2 \cdot 6\text{H}_2\text{O}$ (0.5 mmol) and thiourea (4 mmol) were added into the mixed solution. The mixture was thermally treated at 300 °C for 0.5 h under an argon gas atmosphere, and then the temperature was increased to 600 °C for 1.5 h. The pure Co_9S_8 nanoparticles were prepared through the same procedure but without the additional GO powder.

1.2. Sample characterizations

Phase structure of the samples were studied by using a powder X-ray diffractometer (XRD, Bruker Model D8 Advanced) with Cu K_α irradiation (wavelength $\lambda = 1.5418 \text{ \AA}$). The composition and morphology were characterized by field-emission scanning electron microscopy (FESEM;

Hitachi-S5500, 5 kV). The microstructures of the samples were examined by transmission electron microscopy (TEM; JEOL, JEM-2100, 200 kV). The elemental mapping profiles of the samples were recorded on a Tecnai T20 G² (FEI, 200 kV) equipped with an EDAX system. The chemical compositions, surface valance states as well as nitrogen doping analysis were performed by X-ray photoelectron spectroscopy with Al K α irradiation (XPS, Escalab 250). The existence of few-layer graphene and its content in the sample were determined by Raman microscopy (Renishaw, UK, 633 nm excitation) and thermal gravimetric analysis (TGA, Netzsch-STA 449C). The surface area and pore structure of the samples were analyzed by nitrogen adsorption-desorption isotherm at 77 K (Micromeritics ASAP 2010 system).

1.3. HER tests

The electrocatalytic properties of the samples toward HER were measured in a standard three-electrode glass cell on a Autolab System (Eco Chemie, Netherlands) using a glassy carbon electrode with different catalysts as the working electrode, a graphite rod as the counter electrode, and a KCl-saturated Ag/AgCl as the reference electrode. The electrolyte was made by 0.5 M H₂SO₄ solution (pH \approx 0.31). For the fabrication of the working electrode, the as prepared catalyst powder (\sim 4 mg) was dispersed in N, N-dimethylformamide (DMF, 1 mL). The catalyst ink (3.5 μ L) was dropped onto the glassy carbon electrode (3 mm diameter) and dried naturally. The catalyst loading was \sim 0.2 mg cm⁻². Linear sweep voltammetry (LSV) curves were recorded with a quiet time of 5 s at a sweep rate of 5 mV s⁻¹. The electrochemical AC impedance tests were tested under the bias of -0.35 V (vs. Ag/AgCl) with an AC voltage amplitude of 2 mV from 100 kHz to 0.1 Hz and a quiet time of 2 s. All the current density was normalized by geometric electrode area, and the potential was iR-drop corrected and normalized to reversible hydrogen electrode (RHE)

potential as the following equation: $ERHE = EAPP + E_{Ag/AgCl} + 0.0591 \times pH - iR\Omega$. Herein, $EAPP$ is the applied potential versus $Ag/AgCl$ electrode, and $E_{Ag/AgCl}$ is the electrode potential of KCl-saturated $Ag/AgCl$ (0.197 V vs. standard hydrogen electrode), and $R\Omega$ is the Ohm resistance containing solution resistance and electric curve resistance. Before the electrochemical measurements, the electrolyte was degassed by bubbling nitrogen gas for approximately 30 minutes. All the measurements were performed at room temperature.

1.4. Coin cell assembly and sodium storage performance tests

The working electrodes were fabricated by mixing 80% active materials, 10% conductive carbon black, and 10% carboxymethyl cellulose in Milli-Q water. The slurry-like mixture was spread onto copper foil and dried under vacuum (120 °C, 5 h) to remove the solvent. Then the electrodes were cut into disks and dried in vacuum again (100 °C, 24 h). The CR 2032 coin-type half cells were assembled by using a Na foil as the reference electrode and counter electrode, and microporous polypropylene as the separator. The electrolyte was prepared by dissolving $NaClO_4$ (1 M) in propylene carbonate (PC) with 2 % FEC (fluoroethylene carbonate) additive. The assembled cells were allowed to soak overnight, and then electrochemical tests were recorded on a LAND battery testing unit. Galvanostatic charge and discharge of the assembled cells were performed at different current densities between voltage limits of 0.01 and 3.0 V (vs. Na^+/Na). The cyclic voltammogram (CV) curves of the samples were recorded between 0.01 and 3.0 V (vs. Na^+/Na) at a scan rate of 0.5 mV s^{-1} by using a CHI 660D electrochemical workstation (Chenhua Instrument, Shanghai). Electrochemical impedance spectroscopy (IM6, Zahner) was performed in the frequency range of 100 kHz to 0.01 Hz under open circuit potential by applying a 5 mV AC voltage. All electrochemical tests are performed at room temperature.

2. Supplementary figures

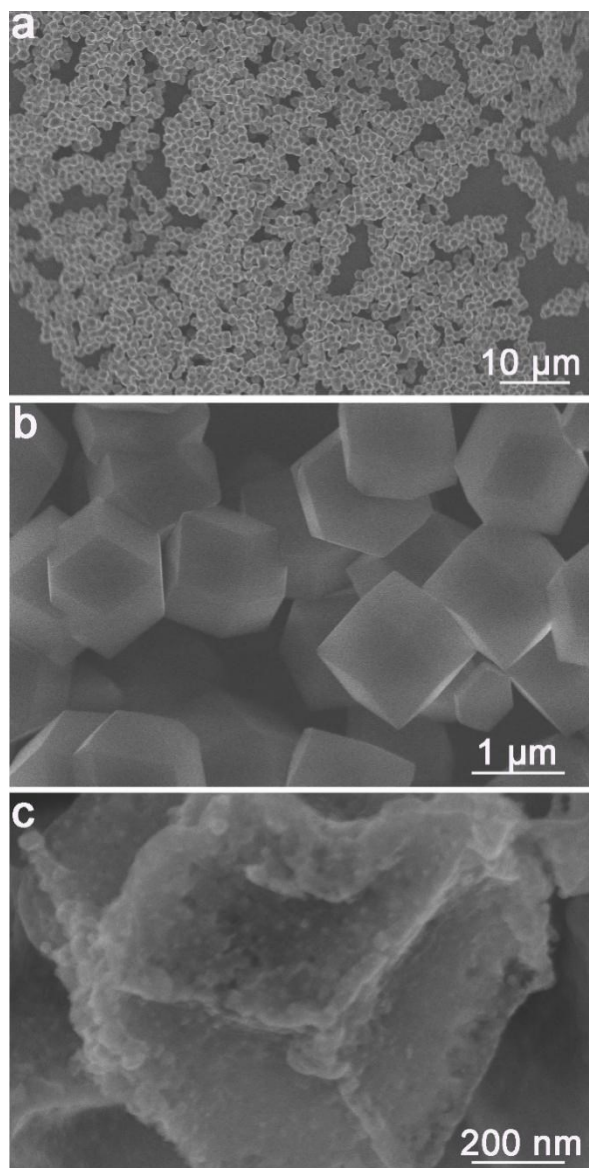


Fig. S1. FESEM images of (a, b) ZIF-67 crystals and (c) CS@NFLG sample.

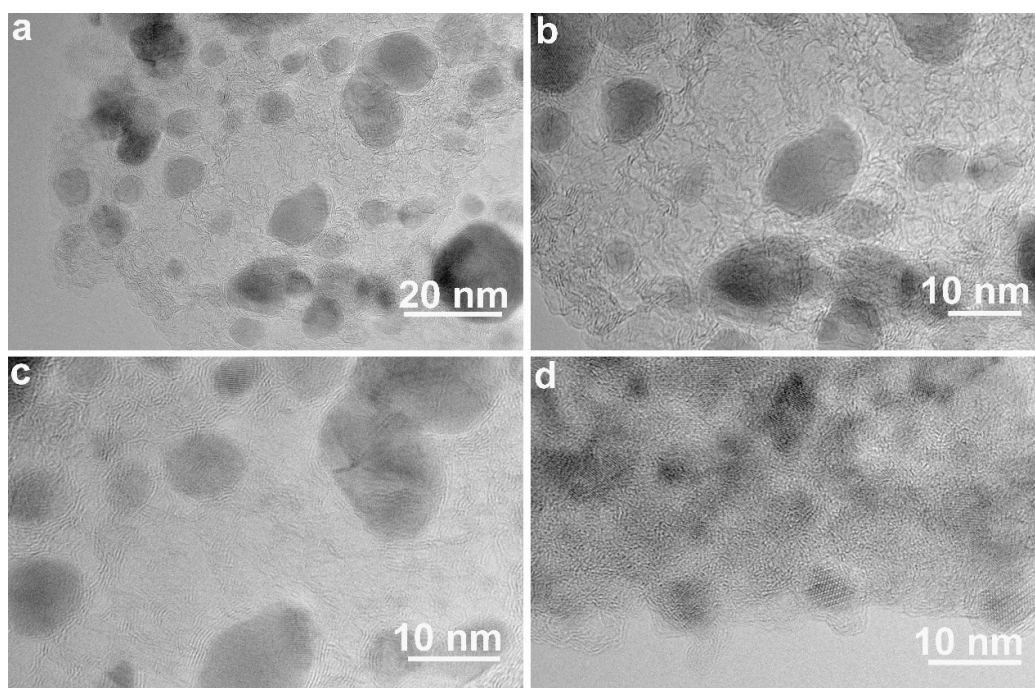


Fig. S2. Additional TEM images of CS@NFLG sample.

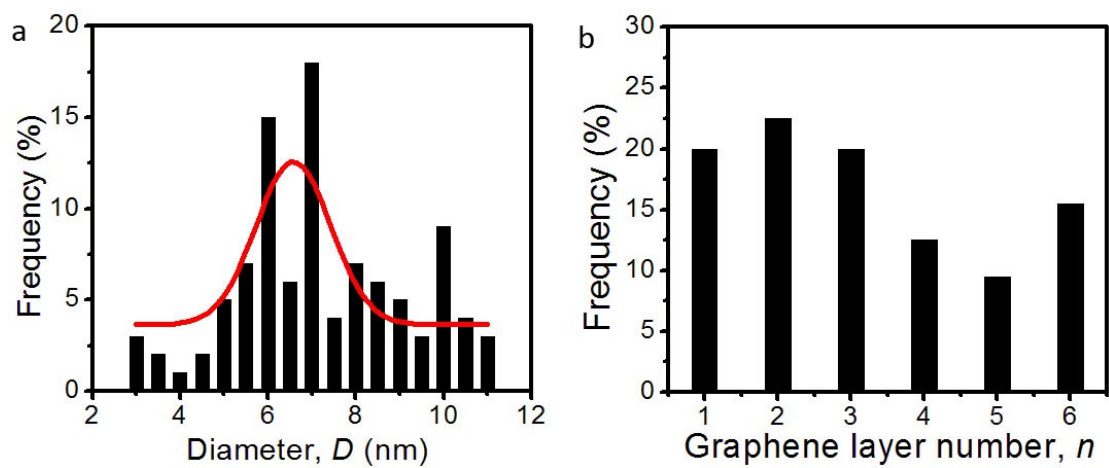


Fig. S3. (a) Size distribution of Co_9S_8 nanoparticles and (b) layer number distribution of graphene in CS@NFLG sample.

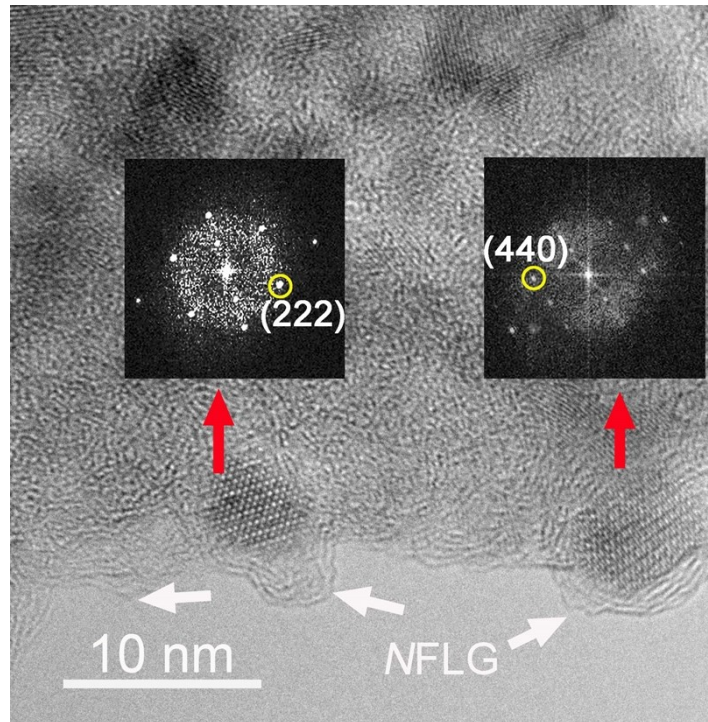


Fig. S4. Additional analysis of Fig. 2f in the main text. The white and red arrows indicate the existence of NFLG and the encapsulated Co_9S_8 particles. The corresponding FFT patterns of Co_9S_8 particles are also shown as the insets.

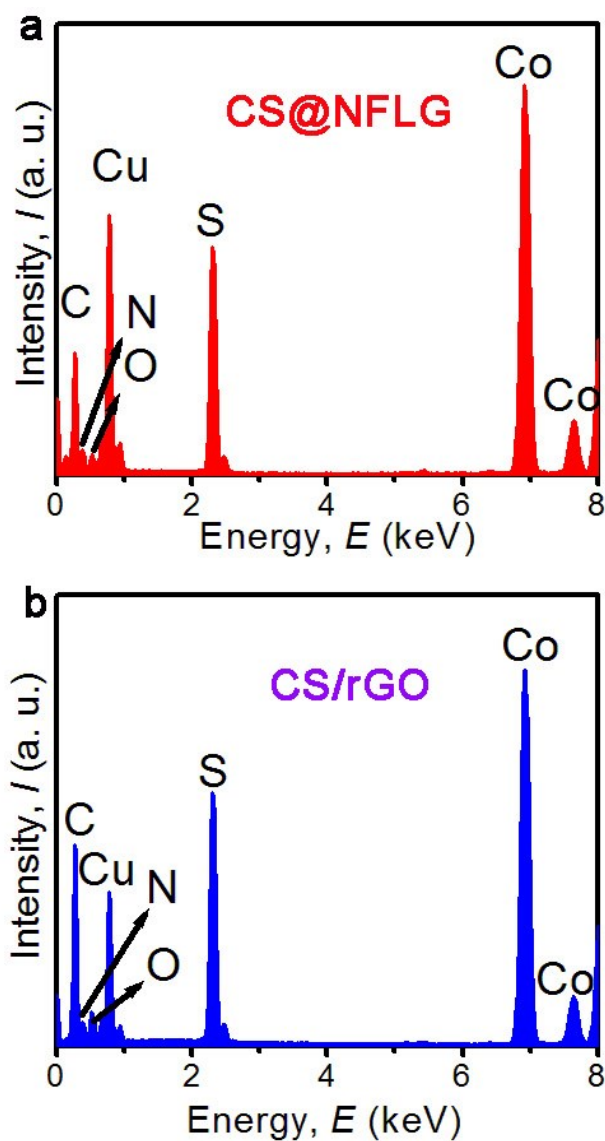


Fig. S5. Energy dispersive X-ray spectroscopy (EDX) patterns of (a) CS@NFLG and (b) CS/rGO samples. Cu signal comes from the copper grid that used to support the sample for TEM observations.

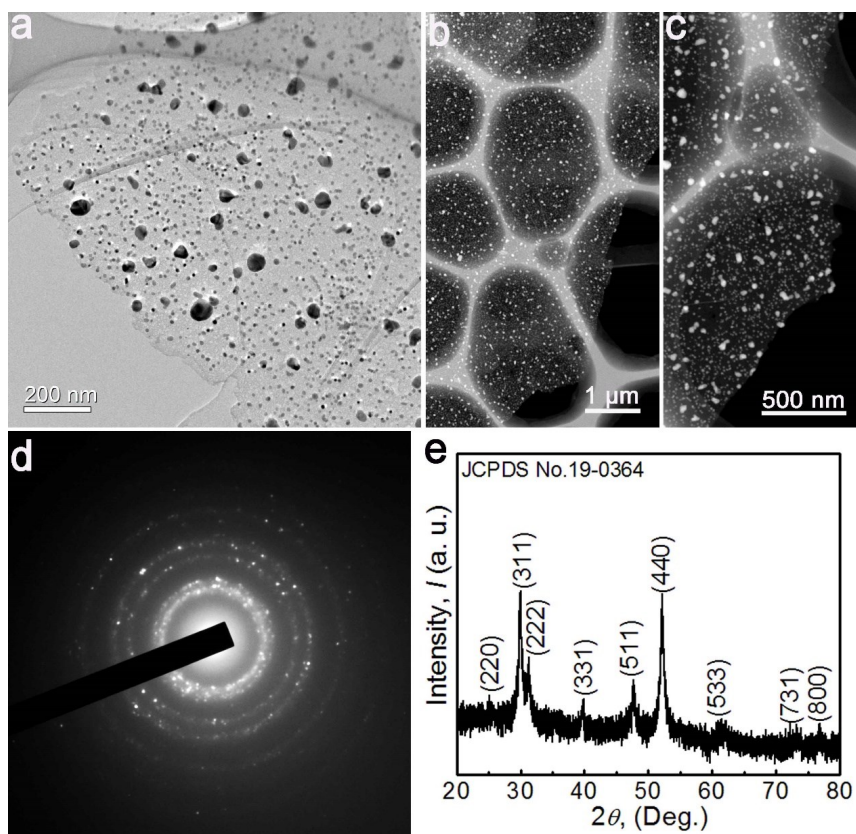


Fig. S6. (a) TEM, (b, c) HAADF-STEM images, (d) SAED and (e) XRD patterns of CS/rGO sample.

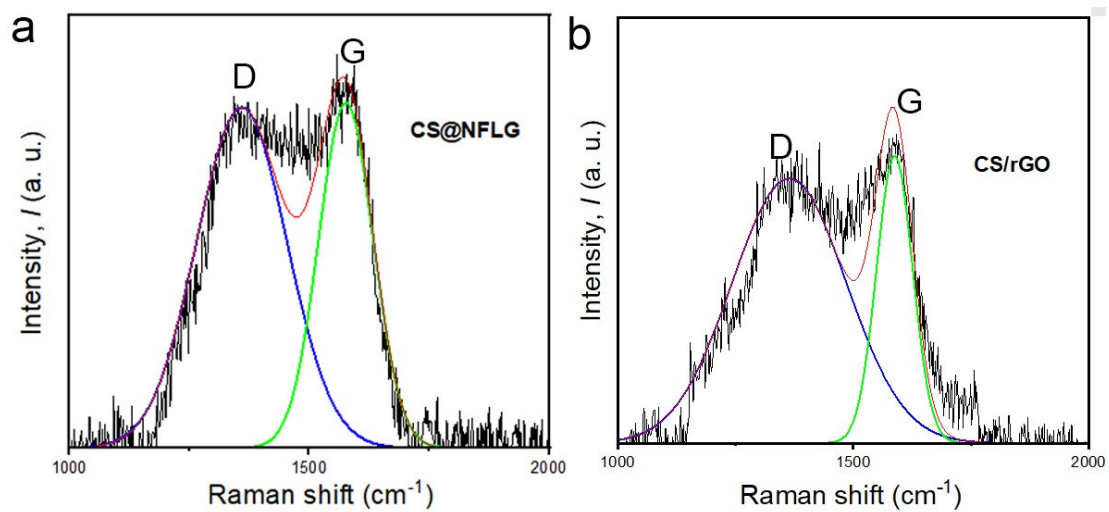


Fig. S7. The enlarged D and G bands of (a) CS@NFLG and (b) CS/rGO samples.

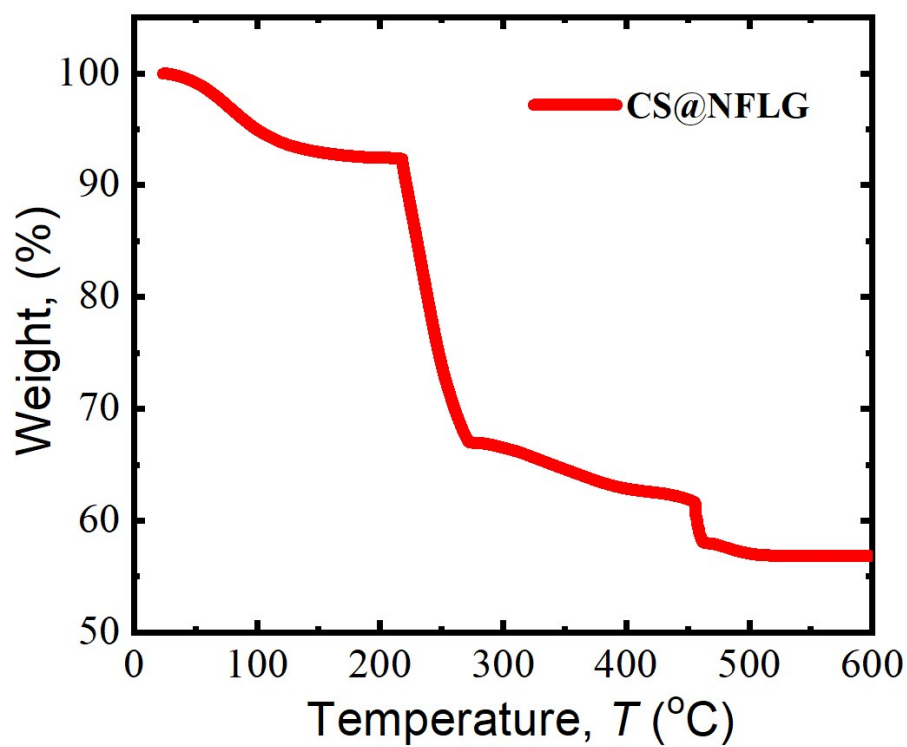


Fig. S8. TGA curve of the CS@NFLG sample measured by using TG 2050 thermogravimetric analyzer under an air atmosphere at the temperature range of 25-600 °C with a heating rate of 10 °C min⁻¹.

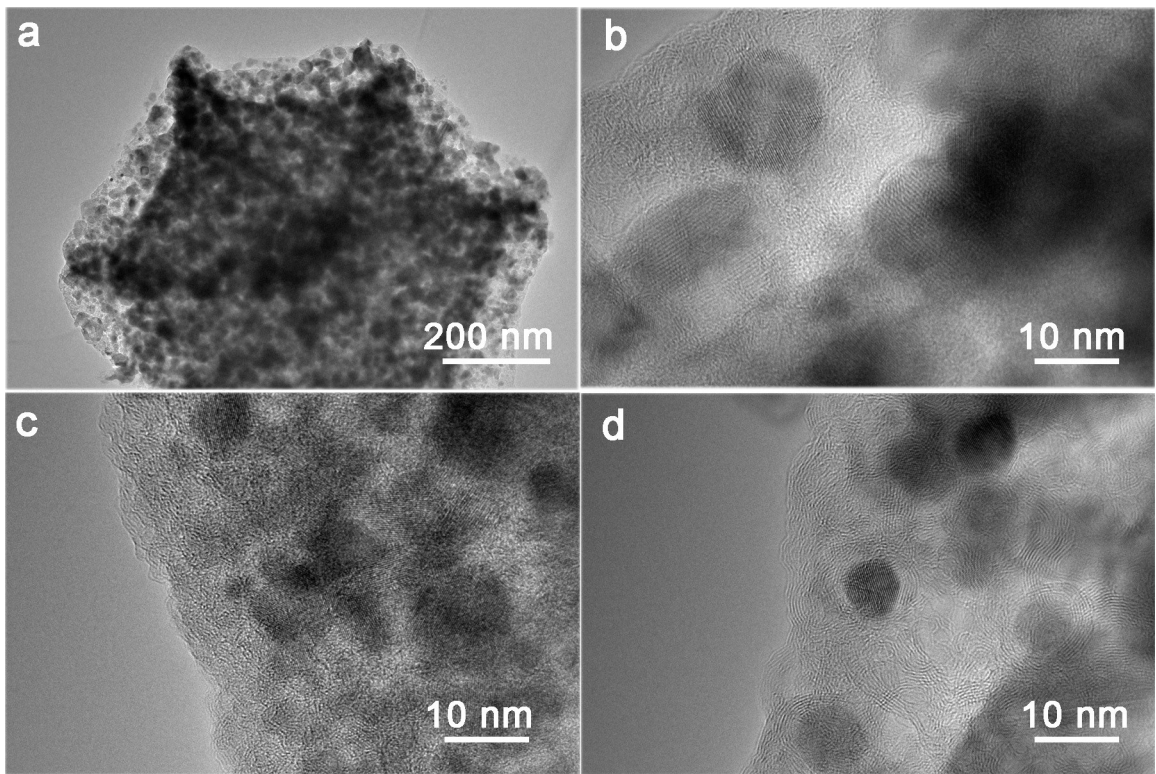


Fig. S9. Typical TEM images of the sample calcinated without trace oxygen.

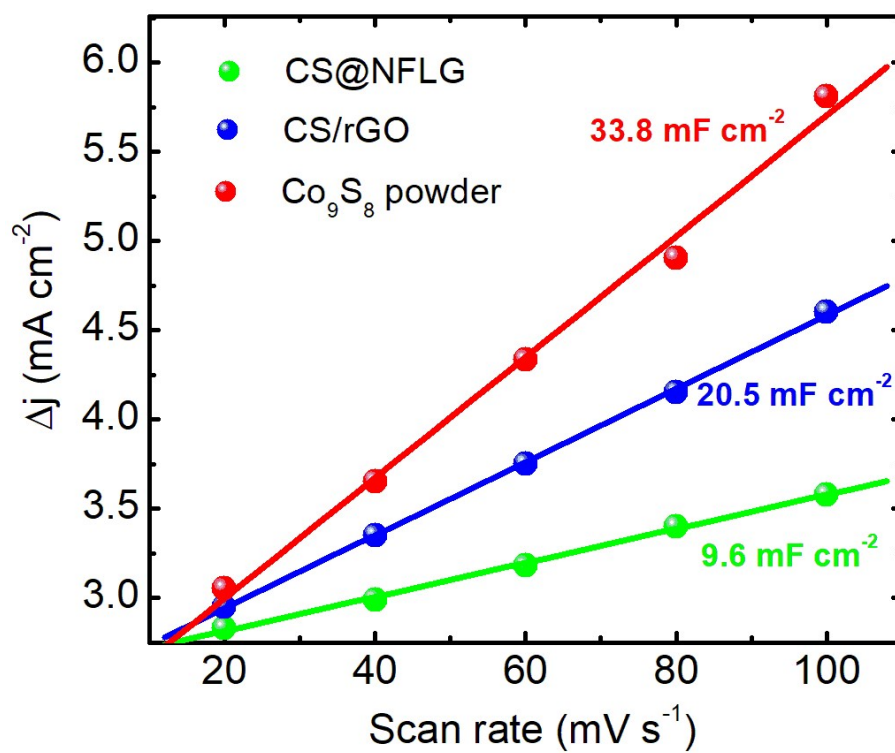


Fig. S10. The capacitive current density Δj at the potential of 0.15 V (vs. RHE) as a function of scan rate.

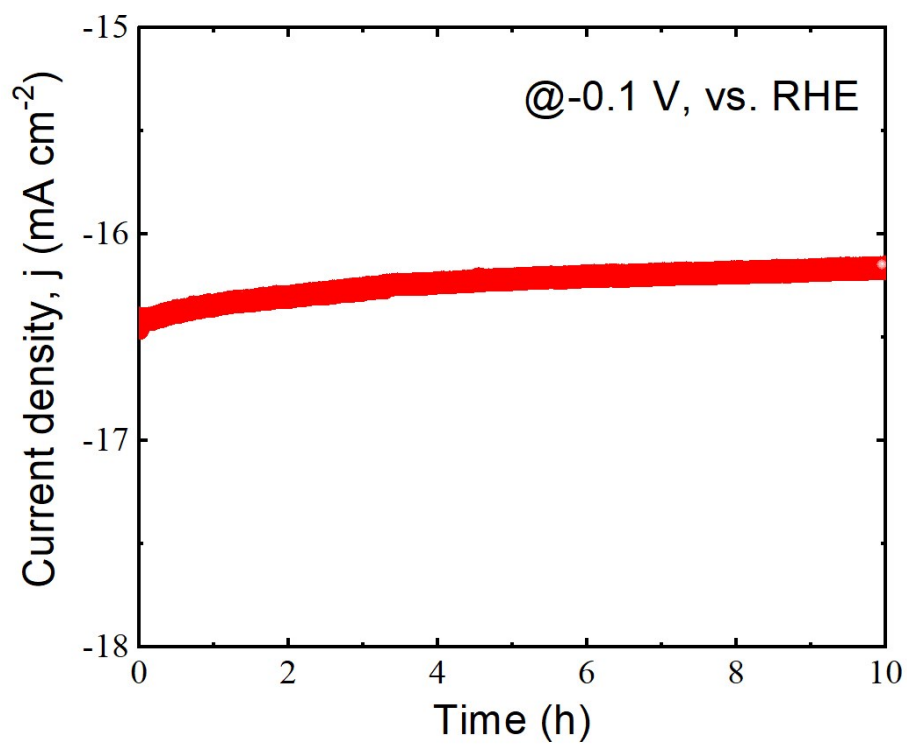


Fig. S11. Chronoamperometric response (i-t) recorded on CS@NFLG sample for 10 h at a constant applied potential of -0.10 V vs. RHE.

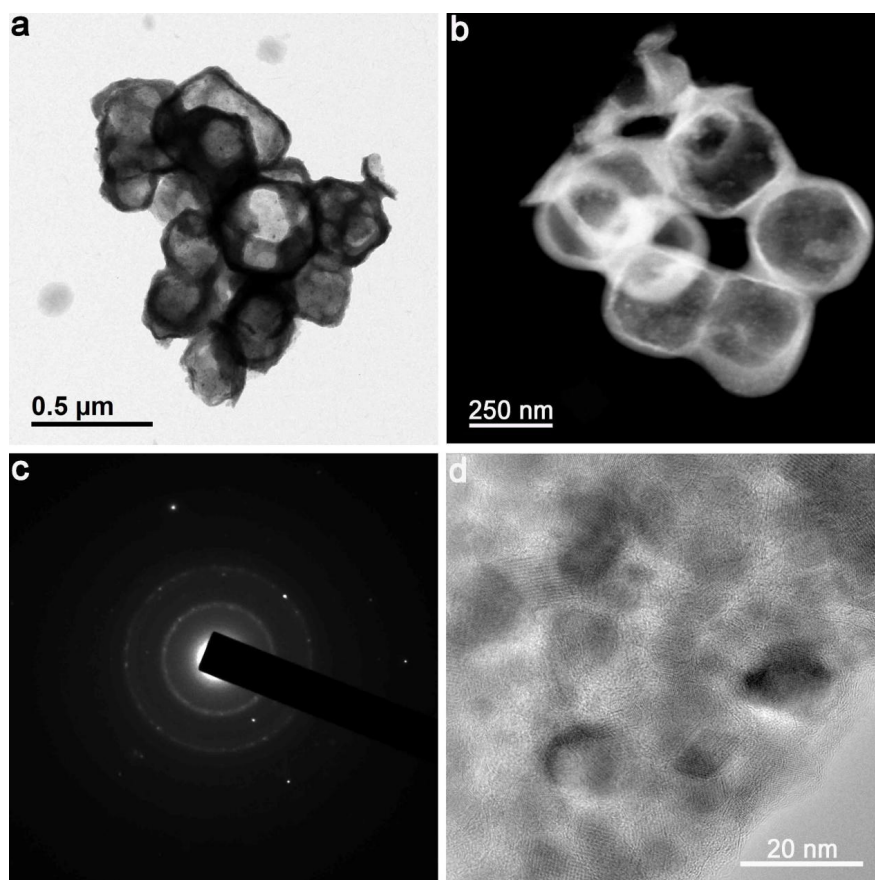


Fig. S12. (a) TEM, (b) HAADF-STEM images, (c) SAED pattern and (d) HRTEM image of CS@NFLG after cycling test.

3. Supplementary tables

Table S1 Comparison of HER properties in acidic media for different Co₉S₈ nanostructures.

Catalysts	Overpotential@10 mA cm ⁻² /mV, vs RHE	Tafel slope /mV dec ⁻¹	Mass loading /mg cm ⁻²	Ref
Co ₉ S ₈ @N-S-HPC	173	78	0.26	1
Co ₉ S ₈ -based nanosheets	—	51	0.38	2
G _{2.0} T _{1.0} Co _{0.3} -900	71	42.4	—	3
TiO ₂ /Co ₉ S ₈ core-branch nanosheet arrays	150	71	—	4
CoS ₂ HNSs	193	100	1.5	5
MoS ₂ -Co ₉ S ₈ -NC	95	77	1.24	6
Co-Co ₉ S ₈ @SN-CNTs -900	—	92	0.8	7
N, S-codoped mesoporous carbon embedded with Co ₉ S ₈ nanoparticles	62	47.3	—	8
Co ₉ S ₈ /MoS ₂ @NSOC	233	96	2.8	9
K-GTC _{0.6} -900	196	75.5	—	10
GTC _{0.900} -KCl/NaCl	131	94.4	—	11
Mo-Co ₉ S ₈ @C	98	34.6	1.0	12
Carbon-armored Co ₉ S ₈ NPs	240	—	0.28	13
Co ₉ S ₈ nanosheets @ carbon cloth	270	—	0.4	14
Co ₉ S ₈ NPs @ N-,O-,S-doped carbon	235	72	0.28	15
Co ₉ S ₈ NPs @ N-,S-doped graphene-CNT	65	84	0.3	16
Co ₉ S ₈ NPs	280	123	0.3	16
Co ₉ S ₈ @MoS _x /carbon cloth	98	64.8	5.8	17
Co ₉ S ₈ /carbon cloth	162	37.6	5.8	17
Fe-doped Co ₉ S ₈ nanosheets/carbon cloth	65	88.1	2.05	18
Co ₉ S ₈ nanosheets/carbon cloth	142	115.3	1.85	18
Co ₉ S ₈ hollow microspheres	250	108	0.8	19
Nanoboxes composed of Co ₉ S ₈ -MoS ₂ Nanosheets	106	51.8	0.21	20
Co ₉ S ₈ -N-S doped C@Mo ₂ C	74	69.3	0.425	21
Co ₉ S ₈ /1L MoS ₂ core/shell nanocrystals	97	71	0.214	22
Co ₉ S ₈ /2L MoS ₂ core/shell nanocrystals	124	92	0.214	22
Co ₉ S ₈ /NFLG networks	88	73	0.23	
Co ₉ S ₈ /rGO	177	95	0.24	this work
Co ₉ S ₈ powder	333	131	0.21	

Table S2 Performance comparison of some SIB anodes based on typical Co₉S₈ structures.

Anodes		Reversible capacity (cycles) /mA h g ⁻¹	Rate capability /mA h g ⁻¹	Voltage window /V (vs. Na ⁺ /Na)	Ref
Carbon-coated nanoparticles	Co ₉ S ₈	320 (30) @ 5 mA g ⁻¹	—	0.5-2.5	23
Co ₉ S ₈ @BNC		388 (100) @100 mA g ⁻¹	258 @ 2 A g ⁻¹	0.01-2.5	24
nickel-doped nanoparticles	Co ₉ S ₈	hollow 556.7 (50) @100 mA g ⁻¹	361 @ 2000 mA g ⁻¹	0.01-3.0	25
Co ₉ S ₈ @C nanospheres		305 (1000) @5 A g ⁻¹	405 @ 500 mA g ⁻¹	0.01-3.0	26
3D Co ₉ S ₈ @CNNs		935 (200) @ 0.25 A g ⁻¹	430 @ 0.05 A g ⁻¹	0.005-3.0	27
carbon-free nanospheres	CoS _x	hollow 572 (100) @ 500 mA g ⁻¹	478.9 @ 2000 mA g ⁻¹	0.01-3.0	28
Co ₉ S ₈ /HNCS		327 (200) @ 500 mA g ⁻¹ 224 (300) @ 1000 mA g ⁻¹	287 @ 2000 mA g ⁻¹	0.01-3.0	29
Co ₉ S ₈ /MoS ₂ -CN		438 (150) @ 1 A g ⁻¹ 421 (250) @ 2 A g ⁻¹	—	0.0-3.0	30
Co ₉ S ₈ @NC-9		458 (500) @ 1000 mA g ⁻¹	629 @ 2000 mA g ⁻¹	0.01-3.0	31
P@Co ₉ S ₈		551.7 (1000) @ 1 A g ⁻¹	478.2 @ 2 A g ⁻¹	0.01-3.0	32
Co ₉ S ₈ @Ni ₃ S ₂		634.2 (100) @1 00 mA g ⁻¹	490 @ 2 A g ⁻¹	0.0-3.0	33
rGO/Co ₉ S ₈		207 (500) @ 5 A g ⁻¹	400 @ 2 A g ⁻¹	0.01-3.0	34
Co ₉ S ₈ @S-CF		373 (1000) @ 0.1 A g ⁻¹	180 @ 20 A g ⁻¹	0.01-3.0	35
3DOM Co ₉ S ₈ -QDs@NC		466 (200) @ 0.1 A g ⁻¹	318 @ 2 A g ⁻¹	0.01-3.0	36
Co ₉ S ₈ @CHSs		492 (100) @ 0.5 A g ⁻¹	462 @ 2 A g ⁻¹	0.25-3.0	37
Co ₉ S ₈ -carbon(C)/Co ₉ S ₈		616 (150) @ 0.5 A g ⁻¹	422 @ 10 A g ⁻¹	0.01-3.0	38
Co ₉ S ₈ @NSC		423 (800) @ 200 mA g ⁻¹	226 @ 5 A g ⁻¹	0.01-3.0	39
Co ₉ S ₈ hollow boxes		520 (100) @ 0.5 A g ⁻¹	253 @ 2 A g ⁻¹	0.25-3.0	40
Co ₉ S ₈ @carbon nanocages	yolk-shell	549.4 (—) @ 0.1 A g ⁻¹	342.5 @ 2 A g ⁻¹	0.2-2.5	41
Co ₉ S ₈ -NC@C		382 (100) @ 100 mA g ⁻¹	280 @ 1000 mA g ⁻¹	0.01-3.0	42
r-Co ₉ S ₈ @NC		483 (150) @ 500 mA g ⁻¹	342 @ 10 A g ⁻¹	0.4-2.8	43
Co ₉ S ₈ -carbon composites		404 (50) @ 500 mA g ⁻¹	511 @ 100 mA g ⁻¹ 326 @ 1500 mA g ⁻¹	0.001-3.0	44
Multi-walled composites	CNTs/Co ₉ S ₈	444 (80) @ 500 mA g ⁻¹	—	0.01-3.0	45
Co ₉ S ₈ /MoS ₂ yolk-shell spheres		373 (80) @ 2000 mA g ⁻¹ 476 (100) @ 300 mA g ⁻¹ 430 (120) @ 1000 mA g ⁻¹ 300 (1200) @ 2000 mA g ⁻¹	— 590 @ 100 mA g ⁻¹ 450 @ 1000 mA g ⁻¹ 423 @ 2000 mA g ⁻¹	0.01-3.0	46
Co _{1-x} S powder		~20 (50) @ 500 mA g ⁻¹	~500 @ 100 mA g ⁻¹ ~0 @ 1500 mA g ⁻¹	0.001-3.0	44
Co ₉ S ₈ powder		10 (30) @ 5 mA g ⁻¹	—	0.5-2.5	23
Co ₉ S ₈ powder		~60 (80) @ 500 mA g ⁻¹	—	0.01-3.0	45

	~30 (80) @ 2000 mA g ⁻¹	—		
Co ₉ S ₈ /NFLG networks	~505 (100) @ 500 mA g ⁻¹	~391 @ 2000 mA g ⁻¹	0.01-3.0	
		1		
Co ₉ S ₈ /rGO	~413 (100) @ 500 mA g ⁻¹	~307 @ 2000 mA g ⁻¹	0.01-3.0	this work
		1		
Co ₉ S ₈ powder	~43 (100) @ 500 mA g ⁻¹	~21 @ 2000 mA g ⁻¹	0.01-3.0	

4. Supplementary references

- [1] S. Zhang, D. Zhai, T. Sun, A. Han, Y. Zhai, W.-C. Cheong, Y. Liu, C. Su, D. Wang and Y. Li, *Appl. Catal. B-Environ.*, 2019, **254**, 186-193.
- [2] X. Zhang, Y. Liu, J. Gao, G. Han, M. Hu, X. Wu, H. Cao, X. Wang and B. Li, *J. Mater. Chem. A*, 2018, **6**, 7977-7987.
- [3] H. Yu, S. Miao, D. Tang, W. Zhang, Y. Huang, Z. A. Qiao, J. Wang and Z. Zhao, *J Colloid Interface Sci*, 2020, **558**, 155-162.
- [4] F. Yang, S. Deng, S. Lin, M. Chen, X. Xia and X. Lu, *Nanotechnology*, 2019, **30**, 404001.
- [5] X. Ma, W. Zhang, Y. Deng, C. Zhong, W. Hu and X. Han, *Nanoscale*, 2018, **10**, 4816-4824.
- [6] N. Huang, S. Yan, M. Zhang, Y. Ding, L. Yang, P. Sun and X. Sun, *Electrochim. Acta*, 2019, **327**, 134942.
- [7] H. Han, Z. Bai, T. Zhang, X. Wang, X. Yang, X. Ma, Y. Zhang, L. Yang and J. Lu, *Nano Energy*, 2019, **56**, 724-732.
- [8] H. Yu, D. Tang, Y. Huang, W. Zhang, X. Sun, X. Yang, Z. A. Qiao, J. Wang and Z. Zhao, *Chempluschem*, 2019, **84**, 1604-1609.
- [9] T.-T. Chen, R. Wang, L.-K. Li, Z.-J. Li and S.-Q. Zang, *Journal of Energy Chemistry*, 2020, **44**, 90-96.
- [10] H. Yu, W. Zhang, S. Miao, Y. Du, Y. Huang, D. Tang, Z.-A. Qiao, J. Wang and Z. Zhao, *Microporous Mesoporous Mater.*, 2020, **302**, 110235.
- [11] H. Yu, X. Sun, D. Tang, Y. Huang, W. Zhang, S. Miao, Z.-A. Qiao, J. Wang and Z. Zhao, *Int. J. Hydrogen Energy*, 2020, **45**, 6006-6014.
- [12] L. Wang, X. Duan, X. Liu, J. Gu, R. Si, Y. Qiu, Y. Qiu, D. Shi, F. Chen, X. Sun, J. Lin and J. Sun, *Adv. Energy Mater.*, 2019, **10**, 1903137.
- [13] L. L. Feng, G. D. Li, Y. P. Liu, Y. Y. Wu, H. Chen, Y. Wang, Y. C. Zou, D. J. Wang and X. X. Zou, *ACS Appl. Mater. Interfaces*, 2015, **7**, 980-988.
- [14] L.-L. Feng, M. Fan, Y. Wu, Y. Liu, G.-D. Li, H. Chen, W. Chen, D. Wang and X. Zou, *J. Mater. Chem. A*, 2016, **4**, 6860-6867.
- [15] S. Huang, Y. Meng, S. He, A. Goswami, Q. Wu, J. Li, S. Tong, T. Asefa and M. Wu, *Adv.*

- Funct. Mater.*, 2017, **27**, 1606585.
- [16] M. Li, H. Zhou, W. Yang, L. Chen, Z. Huang, N. Zhang, C. Fu and Y. Kuang, *J. Mater. Chem. A*, 2017, **5**, 1014-1021.
- [17] X. Zhou, X. Yang, M. N. Hedhili, H. Li, S. Min, J. Ming, K.-W. Huang, W. Zhang and L.-J. Li, *Nano Energy*, 2017, **32**, 470-478.
- [18] K. Ao, D. Li, Y. Yao, P. Lv, Y. Cai and Q. Wei, *Electrochim. Acta*, 2018, **264**, 157-165.
- [19] Y. Zhang, S. Chao, X. Wang, H. Han, Z. Bai and L. Yang, *Electrochim. Acta*, 2017, **246**, 380-390.
- [20] V. Ganesan, S. Lim and J. Kim, *Chemistry-an Asian Journal*, 2018, **13**, 413-420.
- [21] X. Luo, Q. Zhou, S. Du, J. Li, J. Zhong, X. Deng and Y. Liu, *ACS Appl. Mater. Interfaces*, 2018, **10**, 22291-22302.
- [22] H. Zhu, G. Gao, M. Du, J. Zhou, K. Wang, W. Wu, X. Chen, Y. Li, P. Ma, W. Dong, F. Duan, M. Chen, G. Wu, J. Wu, H. Yang and S. Guo, *Adv. Mater.*, 2018, **30**, 1707301.
- [23] X. Liu, H. Liu, Y. Zhao, Y. Dong, Q. Fan and Q. Kuang, *Langmuir*, 2016, **32**, 12593-12602.
- [24] T. Zhang, H. Qu, K. Sun and S. Li, *ChemElectroChem*, 2019, **6**, 1776-1783.
- [25] H. Zhou, Y. Cao, Z. Ma and S. Li, *Nanotechnology*, 2018, **29**, 195201.
- [26] Y. Zhang, N. Wang, P. Xue, Y. Liu, B. Tang, Z. Bai and S. Dou, *Chem. Eng. J.*, 2018, **343**, 512-519.
- [27] X. Zhang, H. Wang and G. Wang, *J Colloid Interface Sci*, 2017, **492**, 41-50.
- [28] Y. Xiao, J.-Y. Hwang, I. Belharouak and Y.-K. Sun, *Nano Energy*, 2017, **32**, 320-328.
- [29] H. Shangguan, W. Huang, C. Engelbrekt, X. Zheng, F. Shen, X. Xiao, L. Ci, P. Si and J. Zhang, *Energy Storage Mater.*, 2019, **18**, 114-124.
- [30] Y. Wang, W. Kang, D. Cao, M. Zhang, Z. Kang, Z. Xiao, R. Wang and D. Sun, *J. Mater. Chem. A*, 2018, **6**, 4776-4782.
- [31] Y. Wu, R. R. Gaddam, C. Zhang, H. Lu, C. Wang, D. Golberg and X. S. Zhao, *Nano-Micro Letters*, 2020, **12**, 48.
- [32] H. Li, Y. Zhang, B. Liu, Z. Gao, G. Zhao, T. Liu, X. Gao, S. Xia and H. Guo, *Sustainable Energy & Fuels*, 2020, **4**, 2208-2219.
- [33] Y. Zhou, J. Zhang, F. Sun, X. Yu, W. Kang and J. Zhang, *J. Solid State Chem.*, 2020, **285**, 121230.

- [34] J. Huang, X. Tang, Z. Li and K. Liu, *J Colloid Interface Sci*, 2018, **532**, 407-415.
- [35] Y. Wang, Y. Wang, Y. X. Wang, X. Feng, W. Chen, J. Qian, X. Ai, H. Yang and Y. Cao, *ACS Appl. Mater. Interfaces*, 2019, **11**, 19218-19226.
- [36] X. Hu, J. Jia, G. Wang, J. Chen, H. Zhan and Z. Wen, *Adv. Energy Mater.*, 2018, **8**, 1801452.
- [37] M. Yin, X. Feng, D. Zhao, Y. Zhao, H. Li, W. Zhou, H. Liu, X. Bai, H. Wang, C. Feng and Q. Jiao, *ACS Sustain. Chem. Eng.*, 2019, **7**, 6122-6130.
- [38] X. Li, K. Li, S. Zhu, K. Fan, L. Lyu, H. Yao, Y. Li, J. Hu, H. Huang, Y. W. Mai and J. B. Goodenough, *Angew. Chem. Int. Ed.*, 2019, **58**, 6239-6243.
- [39] X. Zhang, C. Shang, X. Wang and G. Zhou, *Nanoscale Res Lett*, 2020, **15**, 19.
- [40] M. Yin, D. Zhao, C. Feng, W. Zhou, Q. Jiao, X. Feng, S. Wang, Y. Zhao, H. Li and T. Feng, *ACS Sustain. Chem. Eng.*, 2020, **8**, 6305-6314.
- [41] Y. Zhao, Q. Fu, D. Wang, Q. Pang, Y. Gao, A. Missiul, R. Nemausat, A. Sarapulova, H. Ehrenberg, Y. Wei and G. Chen, *Energy Storage Mater.*, 2019, **18**, 51-58.
- [42] Y. Lian, F. Chen, H. Kang, C. Wu, M. Zhang and S. Xu, *Appl. Surf. Sci.*, 2020, **507**, 145061.
- [43] X. Lin, X. Cui, H. Yan, J. Lei, P. Xu, J. Fan, R. Yuan, M. Zheng and Q. Dong, *ACS Sustain. Chem. Eng.*, 2019, **7**, 15729-15738.
- [44] Y. N. Ko and Y. C. Kang, *Carbon*, 2015, **94**, 85-90.
- [45] H. Zhou and J. Hu, *Mater. Lett.*, 2017, **195**, 26-30.
- [46] H. Geng, J. Yang, Z. Dai, Y. Zhang, Y. Zheng, H. Yu, H. Wang, Z. Luo, Y. Guo, Y. Zhang, H. Fan, X. Wu, J. Zheng, Y. Yang, Q. Yan and H. Gu, *Small*, 2017, **13**, 201603490.